Journal of Colloid and Interface Science 540 (2019) 148–154

Contents lists available at ScienceDirect

Journal of Colloid and Interface Science

journal homepage: www.elsevier.com/locate/jcis

Regular Article

Nanocellulose for gel electrophoresis

Llyza Mendoza, Thilina Gunawardhana, Warren Batchelor, Gil Garnier *

Bioresource Processing Research Institute of Australia (BioPRIA), Department of Chemical Engineering, Monash University, VIC 3800, Australia

GRAPHICAL ABSTRACT

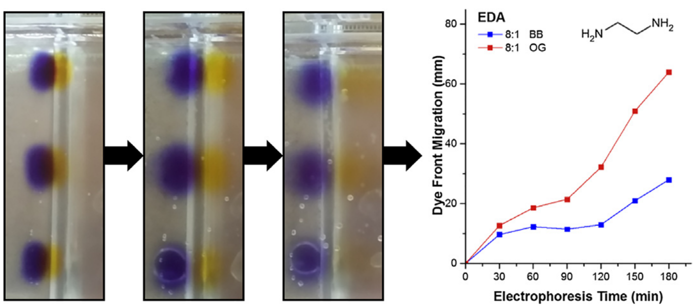

ARTICLE INFO

Article history:
Received 14 December 2018
Revised 3 January 2019
Accepted 4 January 2019
Available online 5 January 2019

Keywords:
Gel electrophoresis
Nanocellulose
TEMPO-mediated oxidation

ABSTRACT

Hypothesis: Cellulose nanofibres produced by TEMPO-mediated oxidation can form gels. This study presents a proof-of-concept for gel electrophoresis with nanocellulose (NC).

Experiments: TEMPO-oxidised cellulose nanofibre dispersion is chemically cross-linked by inducing amide linkages to produce gel slabs for electrophoretic separation. Nanocellulose gel slabs 1 cm thick containing Tris/Borate/EDTA (TBE) buffer were casted. Different cross-linker types and ratios are investigated to assess the migration of conventional electrophoresis tracking dyes.

Findings: Tracking dyes (bromophenol blue and orange G) can diffuse within the gel at different rates and therefore separate. Changing the cross-linker length from EDA to HMDA (C2- to C6-chain) increases the overall network pore size resulting in a faster migration rate for both bromophenol blue and orange G. Increasing the cross-linker concentration stabilises the HMDA-NC gel (no extension) during the electrophoresis run without any effect on the dye migration rate. Increasing the voltage increases the migration rates for both orange G and bromophenol blue. Further development is required to cast the gels evenly and to prevent bubble formation during the cross-linking process. This will enable to effectively separate mixtures of proteins. Nanocellulose gels can become a novel substrate for sustainable biomedical separation and diagnostics by electrophoresis.

1. Introduction

Electrophoresis is a widely used method in molecular biology to separate and identify individual macromolecules from a mixture by the difference in their mobility under an electric field. Negatively charged macromolecules, such as nucleic acids or coated proteins, are fractionated based on their structure, charge, conformation and size as they move towards the anode. Shorter molecules travel faster than longer ones as they can easily migrate through the pores of the gel medium [1]. Initial development of electrophoresis technique began with the work of Arne Tiselius in 1931, separating colloids (human serum) under an electric field [2]. Zone electrophoresis, which utilises substrates such as paper,

* Corresponding author.
E-mail address: gil.garnier@monash.edu (G. Garnier).

https://doi.org/10.1016/j.jcis.2019.01.017

starch, gel, agarose, cellulose acetate or polyacrylamide to act as a sieve to separate a mixture into components as bands, was then developed (1940–1950s) [3]. At present, conventional separation of macromolecules such as DNA or RNA is achieved through agarose and polyacrylamide gels. A mixture of large DNA molecules (200–30,000 bp) [1,4] is often separated through horizontally casted agarose gels because of their larger pores. The neutral charge of the agarose gel network does not interact with the molecules to separate [5]. Separation of smaller protein-based molecules (RNA) (5–1000 bp) [6] is performed typically with a polyacrylamide gel as its pore size is smaller and its structure can better be controlled [7]. However, safety issues arise with the use of the acrylamide monomer as it is classified as a neurotoxin [8,9]. There is a need to develop safer and effective alternatives.

Nanocellulose (NC) fibres are high aspect ratio fibrils derived from cellulose-based sources such as wood or bacteria [10]. Isolation of nanocellulose from various sources can be achieved through a combination of chemical and mechanical processes [11]. One of the most common methods to produce nanocellulose is the TEMPO-mediated oxidation wherein the regio-selective carboxylation of the C6 alcohol of the D-glucose monomer provides the necessary electrostatic repulsion to produce nanofibres upon fibrillation [12]. The combination of nanofibrils with high surface charge and high aspect ratio produces viscous colloidal gels even at low solids content [13].

Studies on the characterisation and application development of nanocellulose have grown exponentially over the last decade. Rheological studies have elucidated their gelation mechanism, achievable property range and even flow instability phenomena [13–18]. Many applications are also being developed ranging from pulp and paper strength additive, agriculture, wastewater to biomedical applications [19–24]. In the biomedical field, nanocellulose composite films and membranes have been developed for protein interaction, passivation and immobilisation for advanced separation purposes [25–30]. Nanocellulose gels have also been used as scaffold structures with tuneable properties suitable for cell culture and tissue engineering [31–34]. Nanocellulose gels were investigated for protein and drug release [35,36]. However, only one study has investigated nanocellulose composite films for electrochemical-based ion-exchange for DNA oligomers [37]. To the best of our knowledge, nanocellulose hydrogels have never been studied as an electrophoretic material before.

This study investigates the potential of nanocellulose gels as electrophoresis substrates. Gel slabs are casted by chemically cross-linking nanocellulose fibres with diamine cross-linkers. The effect of cross-linker properties such as chain length and concentration on the migration of two model tracking dyes is evaluated. The effects of electrophoresis conditions (voltage) on the migration behaviour are also studied. The last section presents a perspective of nanocellulose gels development for DNA and protein mixture separation.

2. Methodology

2.1. Materials

A 0.82 wt% TEMPO-oxidised cellulose nanofibre suspension (containing 1.5 mmol COO^-/g fibre) was purchased from the Process Development Center, University of Maine. Hexamethylenediamine (HMDA) and ethylenediamine (EDA) were bought from Sigma-Aldrich. Glycerol, Orange G and Bromophenol blue was purchased from Merck. Tris/Borate/EDTA (TBE) 10x buffer was bought from Bio-Rad. All chemicals were used as received and were analytical grade.

2.2. Formulation and casting of nanocellulose gel slabs

A 50 mL nanocellulose suspension is mixed with 5 mL 10x TBE buffer under nitrogen gas. The cross-linker (EDA or HMDA) is then added rapidly under thorough agitation. Once a uniform colour is reached, the suspension is immediately poured in a 7 cm × 10 cm transparent gel caster (Bio-Rad Sub-Cell GT UV Transparent Mini-Gel Tray). The gel is then cured at 80 °C for 1 h in an oven. The cross-linked gel is taken out of the oven and cooled at 4 °C. The sample wells are then stamped before running an electrophoresis experiment. Table 1 summarises the ratio of amine to carboxylate group studied:

Nanocellulose gels cross-linked with EDA and HMDA are referred to as EDA-NC and HMDA-NC, respectively.

2.3. Electrophoresis experiments

Electrophoresis was performed using a Bio-Rad Wide Mini Sub-Cell GT system. The gel is submerged in 1x TBE buffer. Samples (tracking dyes) were loaded at various sample wells of the gel. The tracking dye was prepared by mixing the following: 0.25 g bromophenol blue, 0.15 g Orange G, 6 mL 50% glycerol, 4 mL milliQ water. Tracking dyes were utilised to monitor the progression of electrophoresis. Orange G represents the smaller protein molecules and hence migrates faster in contrast to bromophenol blue. The 0.2 mL formulated tracking dye is diluted to a total 1 mL prior to electrophoresis. 20 μL of the dilute tracking dye was added in 3 different regions (left, centre, right) in the gel. The voltage is set at various levels (50, 75, and 100 V) for the electrophoresis to start. The migration rate of tracking dye front is measured visually by the naked eye at 30-minute intervals, for at least 3 h or until the orange G dye reached the end of the gel.

2.4. Characterisation of cross-linked nanocellulose

The characterisation of the cross-linking reaction is performed through ATR-FTIR using the Agilent Cary 630 FTIR Spectrometer. The gels are firstly frozen at −80 °C then freeze-dried to sublimate all of the water. The HMDA-/EDA-NC samples ground and then tested for the FTIR spectra (4000–450 cm^{-1}).

3. Results

3.1. Gel cross-linking by boric acid-catalysed amide formation

Nanocellulose gel slabs were prepared through boric acid catalysed amide formation between the carboxylate groups of nanocellulose and amine groups of di-amine cross-linkers followed by 80 °C curing. The appearance of amide bonds, indicating the cross-linking of nanocellulose gel slabs, is shown in the FTIR spectra (Fig. 1). The spectra of the neat nanocellulose gel displays the representative peaks of the pendant carboxylate group (COO^-) 1601 cm^{-1} corresponding to the C=O stretch, respectively. The C=O stretch peak shifts in the amide cross-linked gels for both HMDA-NC and EDA-NC gels. Curing the gels at 80 °C produces larger peaks at all areas of interest. Fig. 2 shows a cross-linked 8:1 EDA-NC gel.

Table 1
Cross-linker type and ratios for the different casted nanocellulose gel slabs.

Cross-linker type	Ratio (mol NH_2: mol COO^-)
EDA (C2)	8:1, 12:1
HMDA (C6)	4:1, 6:1, 8:1

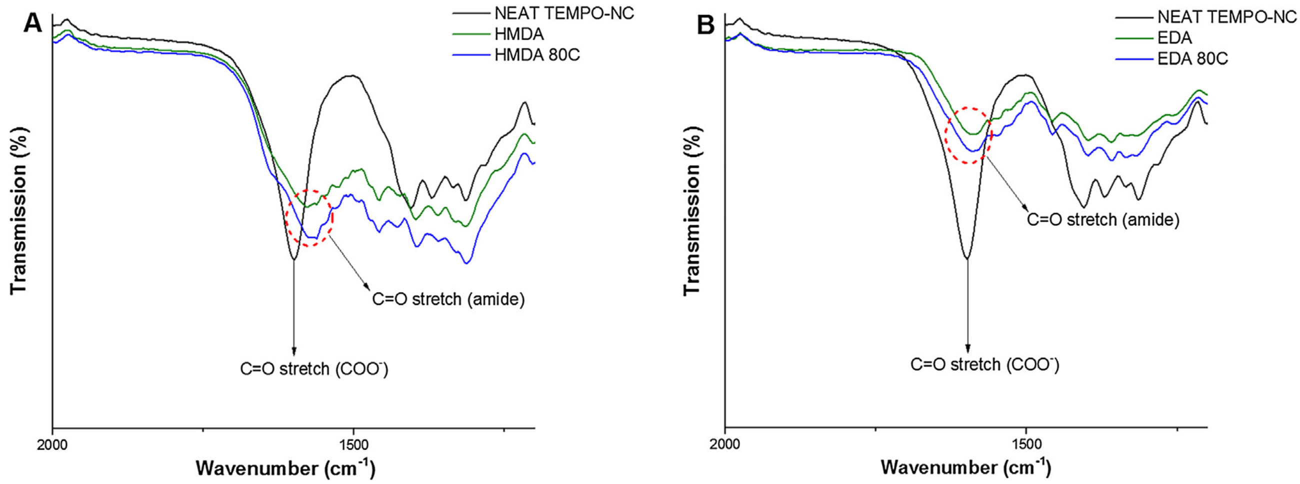

Fig. 1. FTIR spectra evolution of cross-linking of nanocellulose gel slabs with 8:1 (A) HMDA and (B) EDA. Room temperature and 80 °C reactions catalysed by boric acid.

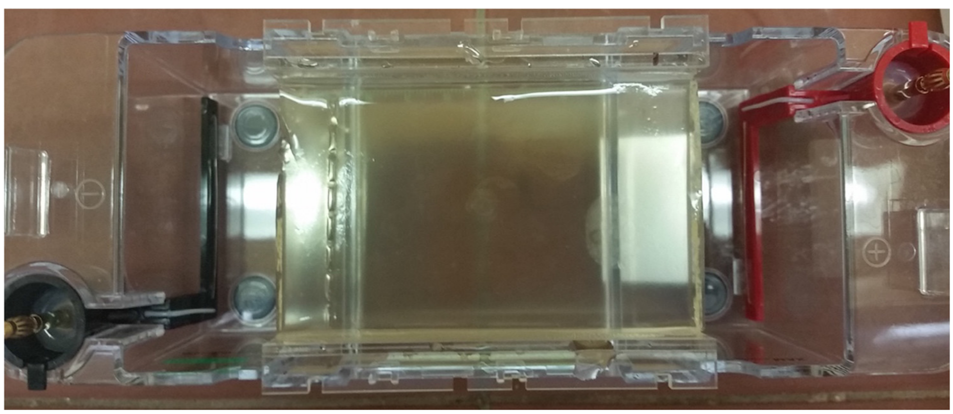

Fig. 2. A casted 8:1 EDA-NC gel placed on a horizontal electrophoresis system.

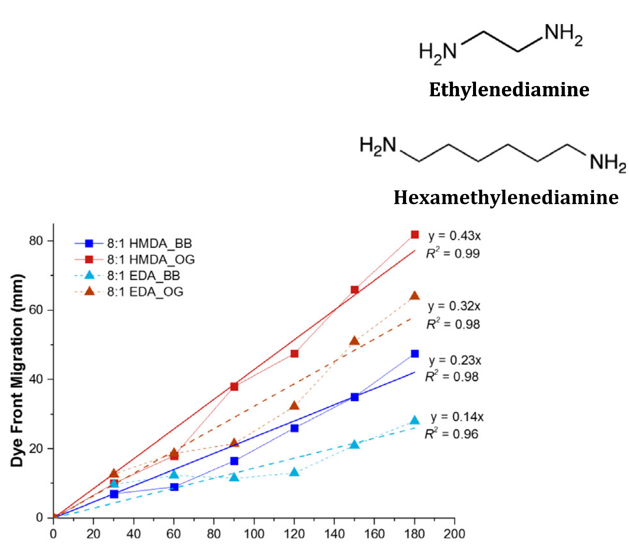

Fig. 3. Migration of Bromophenol Blue (BB) and Orange G (OG) dyes in HMDA-(8:1) and EDA-(8:1) cross-linked nanocellulose gel slabs. Bold lines indicate trend lines and faint lines indicate the actual migration behaviour of tracking dyes. Chemical structures of EDA and HMDA. Electrophoresis voltage constant at 100 V.

3.2. Effect of the cross-linker chain length

The amine-crosslinkers used in this study vary in the length of the carbon backbone. Ethylenediamine (EDA) is a C2-chain whereas hexamethylenediamine (HMDA) has a 6-carbon chain. The effect of amine cross-linker chain length (C2 vs C6) on the migration rate of the tracking dyes in the nanocellulose gel is shown in Fig. 3. Images of EDA- and HMDA-NC gels at different time intervals during electrophoresis are shown in Fig. 4 and supplementary information, respectively. The migration rate of both tracking dyes decreases in EDA-NC compared to HMDA-NC. The migration of bromophenol blue reduces from 0.23 to 0.14 mm min^{-1} (at 100 V). Similarly, orange G travels at a rate of 0.43 mm min^{-1} in HMDA-NC whereas it slows down to 0.32 mm min^{-1} in EDA-NC. Moreover, migration behaviour differs between the two cross-linker types. In HMDA-gels, the tracking dyes travels more linearly throughout the electrophoresis run. The tracking dye behaviour in EDA-NC gels is less linear as a plateau region is observed between 60 and 120 mins.

3.3. Effect of cross-linker concentration

Fig. 5 shows the effect of cross-linker concentration on the mobility of bromophenol blue and orange G during electrophoresis for EDA-NC and HMDA-NC gels. For both cross-linker types, the

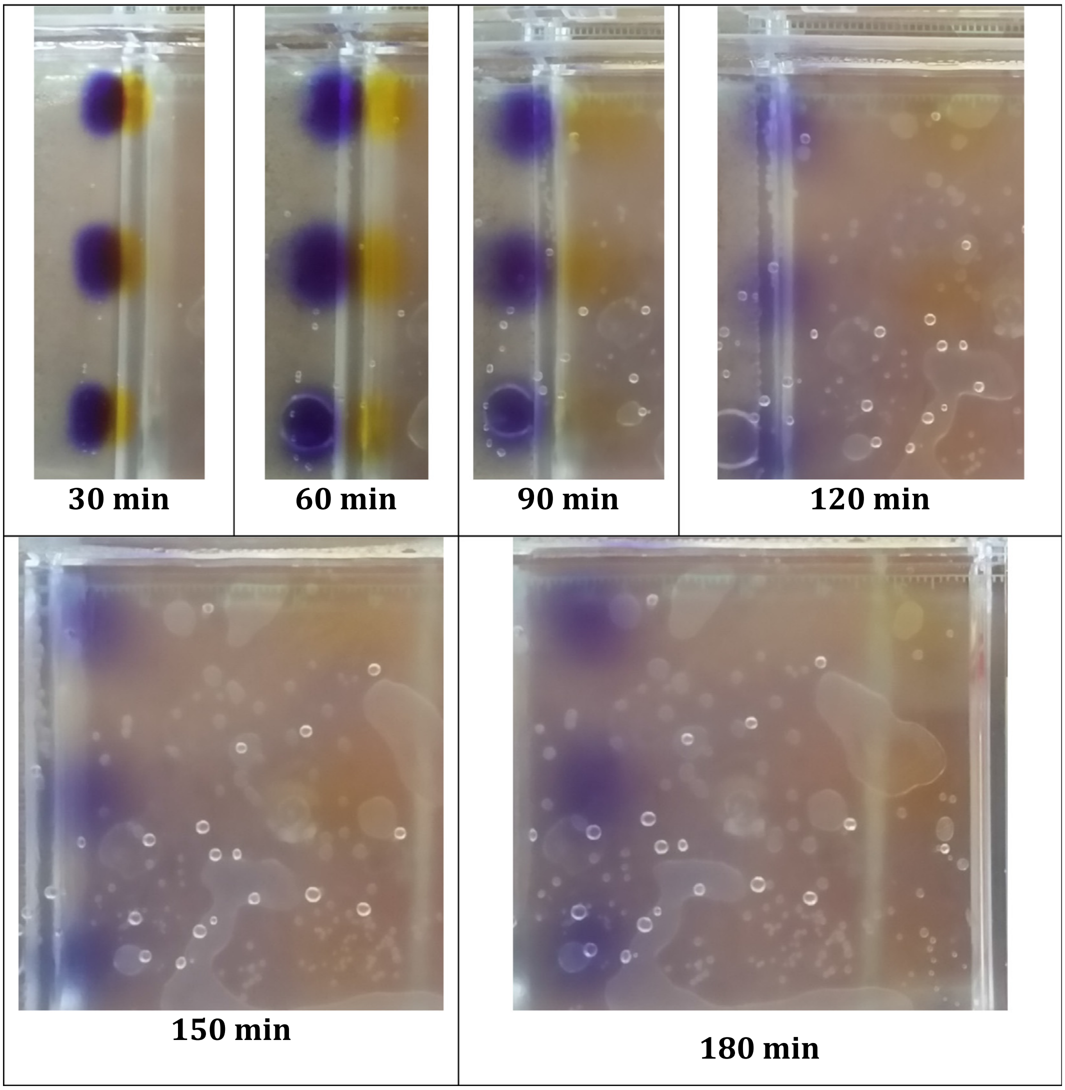

Fig. 4. Migration of Tracking Dyes at 30 min intervals in 8:1 EDA-NC gel. Electrophoresis voltage constant at 100 V.

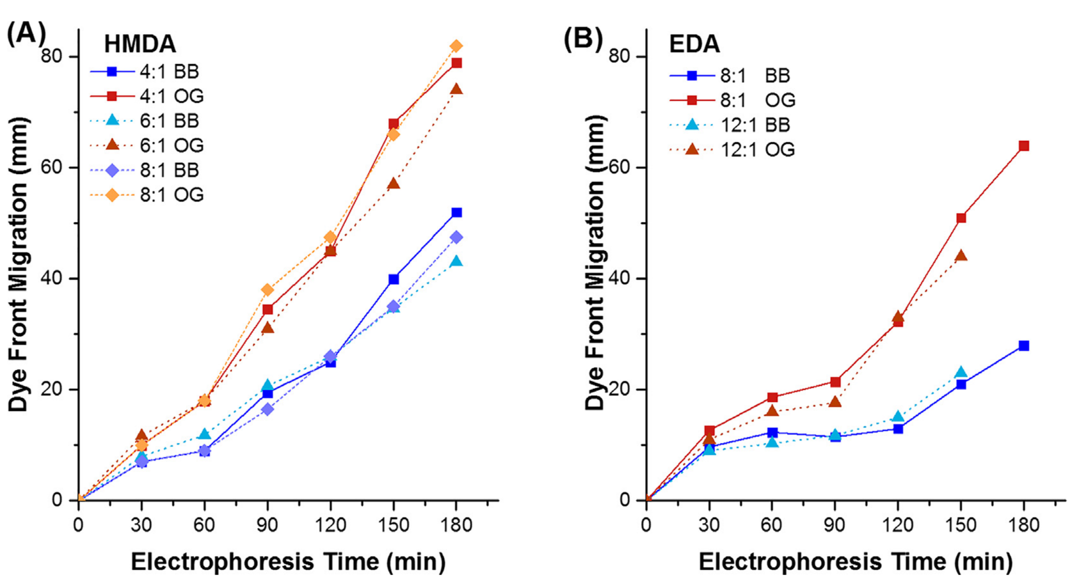

Fig. 5. Migration of Bromophenol Blue (BB) and Orange G (OG) in a (A) HMDA cross-linked and (B) EDA cross-linked nanocellulose gel at various NH_2: COO^- concentrations. Electrophoresis voltage constant at 100 V.

increase in the cross-linker concentration has no effect on the migration behaviour and rate of either bromophenol blue or orange G. Gel stability and ease of handling however increases with cross-linker concentration, particularly with HMDA. All gels tested become increasingly stiffer with higher cross-linker concentration. Increasing the cross-linker concentration from 2:1 onwards maintains gel stability throughout the electrophoresis run. However, all EDA-NC gels tested are very unstable with the gels extending and retracting at both sides of the cell during electrophoresis.

3.4. Effect of electrophoresis voltage

Varying the electrophoresis voltage changes the migration rate for 8:1 HMDA-NC gel as shown in Fig. 6. Increasing the voltage from 50 V to 100 V results in almost tripling and doubling the migration rate of orange G and bromophenol blue, respectively. Moreover, the separation gap between both dyes becomes larger with increasing voltage.

4. Discussion

4.1. Gel cross-linking and gel slab formation

TEMPO-oxidised cellulose nanofibres (TOCNs) can form a suspension or colloidal gel depending on the combination of fibre length and concentration [13,38]. The nanocellulose suspension selected in this study has a concentration of 0.82 wt% and still exhibits primarily liquid-like behaviour. At this initial state, the nanocellulose fibres are not sufficiently entangled to form the stable 3D-network of a gel. Introducing cross-links is therefore necessary to produce a uniform gel slab which remains stable under electrophoretic conditions.

TOCNs contain COO^- groups which can be cross-linked to improve dimensional stability and form a stable gel. Cross-linking can be achieved either by physical or chemical means [39]. Physical cross-linking of TEMPO-nanocellulose can be accomplished with divalent (Ca^{2+}, Zn^{2+}, Cu^{2+}) or trivalent (Al^{3+}, Fe^{3+}) cations which coordinate with the COO- groups to induce chain-chain association similar to pectins and alginates. This results in very stiff gels [40]. These cations, however, are prone to movement and can leave the gel upon the introduction of electrical current. This can lead to gel instability and collapse. Moreover, as the individual fibres are not completely neutralised in this type of cross-linking, their negative charges induce nanocellulose fibre migration during electrophoresis. Temperature and pressure have recently been reported as a trigger for nanocellulose gelation. Nonetheless, the increased gel strength and stability achieved may not be sufficient for electrophoresis operations [41,42].

Chemical cross-linking, on the other hand, provides a more stable network as the fibres are permanently bridged with a cross-linker. Carboxylic acid groups in different substances can be bridged by amine-based cross-linkers to induce amide bond formation. Amide formation is not spontaneous under ambient conditions as the carboxylic acid is deprotonated to form an ammonium carboxylate salt. Conversion to amide requires heat to overcome the activation energy with water as a by-product to be driven off for the reaction to progress [43]. Hence, when either EDA or HMDA is added to TOCNs at ambient conditions, no cross-linking occurs.

Different catalysts and co-reactants are required to produce amides at ambient conditions. For instance, coupling agents such as 1-ethyl-3-(-3-dimethylaminopropyl) carbodiimide (EDC) combined with *N*-hydroxysuccinimide (NHS) is a common reaction system [44]. Boric acid, a component in DNA electrophoresis buffers, can also act as a catalyst to trigger carboxylate group – amine cross-linking to produce amide bonds [45,46]. Amide formation in TOCNs with boric acid is triggered at room temperature as shown in Fig. 1. The change in the representative spectra of COO- groups indicates the formation of amide bonds at room temperature. Full conversion is not achieved as a stronger FTIR signal is shown after the gel is cured at 80 °C for 1 h. This increased amide formation is also demonstrated by the higher stability and ease of handling of the cured gel.

4.2. Effect of cross-linker type

The effect of two types of diamine cross-linkers on the gel slab formation and tracking dye migration behaviour is investigated. Ethylenediamine (EDA) and hexamethylenediamine (HMDA) are both diamine compounds which only differ in the length of the hydrocarbon backbone. EDA and HMDA consist of 2 and 6 carbon chain, respectively. The cross-linker chain length determines the cross-linking likelihood, bond rigidity, and average pore mesh of the resulting three-dimensional network formed by the

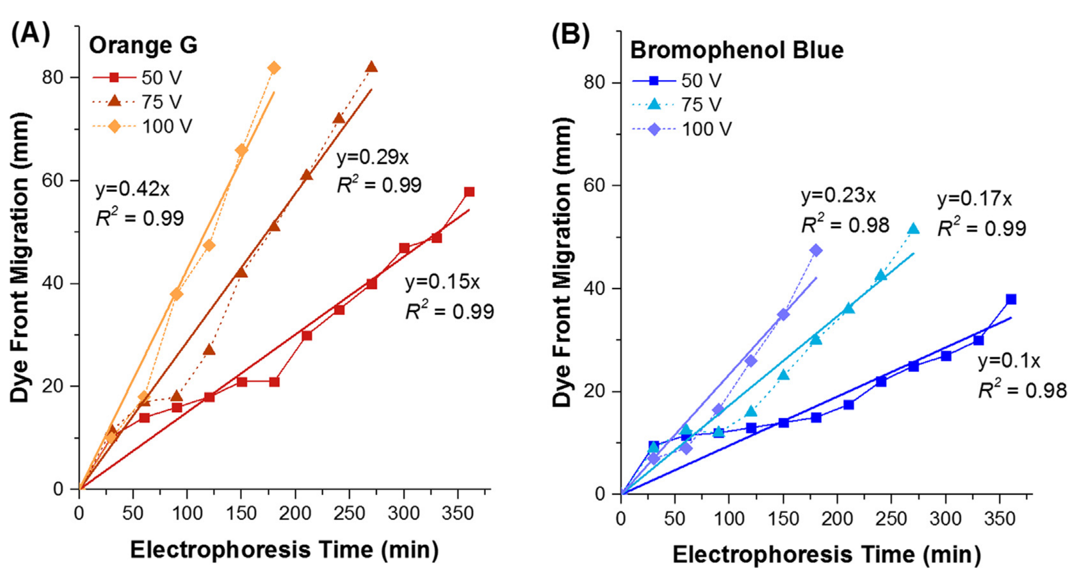

Fig. 6. Migration of (A) Orange G (OG) and (B) Bromophenol Blue (BB) in an 8:1 HMDA cross-linked nanocellulose gel at different electrophoresis voltages. The linear trendlines were added with a y-intercept set at zero. The slope represents the average migration rate under various voltages.

nanocellulose fibres. A longer cross-linker is able to bridge more effectively individual nanocellulose fibres separated by repelling electrostatic forces. It is therefore expected that a longer chain cross-linker will produce a more stable gel. HMDA-NC gels are stronger than EDA-NC gels, similarly reported in [47]. In this investigation, we extend the idea of stability from just producing a self-standing gel to maintaining its structural integrity whilst immersed in an electrophoretic environment. At constant NH_2: COO^- ratio of 8:1, EDA-NC gels extended and contracted at different time periods throughout the electrophoresis experiment. This is in contrast with HMDA-NC which remains unchanged. The change in gel shape (extension and contraction) can be attributed to the lack of stiffness of EDA-NC gels as fibre mobility is less restricted than for HMDA-NC gels. Another reason might be that the diamine terminated cross-linkers have not fully formed amide bonds at both ends, resulting in a net positive charge on the fibre surface leading to the increased electrophoretic movement observed.

The migration rate and behaviour of orange G and bromophenol blue are also affected by HMDA and EDA. Both tracking dyes display lower migration rates in EDA-NC gels. The small chain length in EDA resulted in smaller network pores upon cross-linking in contrast to HMDA. The change in the cross-linker length impacts the migration rate as it decreases by 25.6% and 39.1% in orange G and bromophenol blue, respectively. Moreover, non-linearity in the dyes migration rates are observed for EDA-NC gels. A plateau region in the electrophoresis run is observed wherein there is very little movement (Fig. 3). This can be attributed to the movement of the tracking dyes relative to the gel dimensional instability (extension) resulting in net zero movement.

4.3. Effect of cross-linker concentration

Modifying the cross-linker concentration (NH_2: COO^- ratio) influences the stability of the gels. The higher cross-linker concentration for HMDA-gels forms gel slabs which are more stable: they are easier to handle (i.e. stronger) and do not deform (no dimensional extension) during the electrophoresis testing. This is due to the formation of more crosslinking junctions. However, for EDA-gels, increasing the cross-linker concentration does not improve the gel stability during electrophoresis. Gel extension is still observed even at higher cross-linker concentrations (12:1). Furthermore, the amount of cross-linker concentration does not affect the migration rate of the tracking dyes (Fig. 5). For all HMDA gels (4:1 to 8:1), the tracking dyes travel at similar rates. Similarly, the migration behaviour in EDC gels does not change significantly. This indicates that the network pore sizes have not changed significantly with the increase in cross-linker concentration.

4.4. Effect of electrophoresis voltage

The electrophoresis voltage dictates the migration rate and the degree of separation between molecules and dyes. A higher electrophoresis voltage indicates a faster migration rate which may affect the quality of separation as it can cause smearing or distortion of bands. In cross-linked nanocellulose gels, the tracking dyes travels the slowest at 50 V and fastest at 100 V (Fig. 6). Doubling the voltage from 50 V to 100 V results in tripling of the migration rate of orange G and doubling for bromophenol blue. Moreover, at increasing voltage the gap between orange G and bromophenol blue increases.

4.5. Development perspectives

There are four main development issues to resolve for consistent and effective separation with nanocellulose gel electrophoresis:

- *Bubble formation during casting.* The presence of bubbles can inhibit the effective separation of tracking dyes or proteins due to the absence of current within the bubbles in contrast to the gel which carries the current. Distortion of the separation bands was observed as the dyes are dragged around the bubbles. Hence, there is a need to engineer casting methods to suit nanocellulose gels which may include mixing under vacuum prior to gelation. A well stamp can also be integrated with the caster upon curing such that wells are always well-formed.
- *Nanocellulose gels for substitution of SDS-PAGE.* Trials on casting ultra-thin (0.75 mm) nanocellulose gels to mimic SDS-PAGE (sodium dodecyl sulphate-polyacrylamide gel) for RNA separation were attempted. Concentrated solutions of Al^{3+} and Ca^{2+} cations, which are known to physically cross-link nanocellulose gels, were each applied to the casting plate via plasma-coating and spin-coating techniques. However, uneven precipitation of cations and SDS-nanocellulose interactions prevented even gelation.
- *Investigation of kinetics.* The kinetics and extent of the amide cross-linking reaction can be investigated to optimise casting methods.
- *Optimisation of nanocellulose type.* Nanocellulose properties such as aspect ratio and surface charge can be modified for optimisation of the pore size network to enable enhanced separation. This is best achieved by testing gels from cellulose nanocrystals and bacterial cellulose.

5. Conclusion

Nanocellulose gels have been increasingly studied for applications spanning agriculture [20,21], personal care and hygiene [48], biomedicine [10,31,34] and drug delivery media [35]. In this study, we report a proof-of-concept for utilising nanocellulose gels as novel electrophoresis media. Nanocellulose gels were investigated as an electrophoretic material by understanding the fundamentals which govern electrophoretic separation. Gels from TEMPO-oxidised cellulose nanofibres were chemically cross-linked by diamines to form slabs for horizontal gel electrophoresis. We demonstrated the feasibility of boric acid catalysed amide formation between the carboxylate pendant groups of the nanocellulose fibres with diamine terminated cross-linkers. Curing (80 °C) enhanced the cross-linking for increased gel stability (handleability and minimal deformation during electrophoresis). The pore size of the gel network was varied with the carbon chain length of the diamine cross-linker molecule. This affected the migration rates for both the bromophenol blue and orange G dyes. Gel stability was also influenced as shorter cross-linkers (i.e. EDA) produced unstable gels which extend and retract at both ends of the cell during electrophoresis; this is due to incomplete junctions of the short diamine and the lack of gel stiffness. Increasing the cross-linker concentration increased gel stability and handleability whilst migration rate and behaviour remained constant. Increasing the electrophoresis voltage increased the migration rate and separation gap between bromophenol blue and orange G. Further optimisation is required for developing nanocellulose gels as robust and consistent electrophoretic materials. This especially involves process improvement for producing bubble-free and homogeneous gels. Nanocellulose gels have the potential to become the next generation of efficient and safe electrophoretic media for biomolecule separation.

Acknowledgments

This work was funded by the ARC Bioprocessing Advance Manufacturing Industry Research Transformation (BAMI) Hub IH13100016, Visy, Norske Skog, Orora, CHH/Oji Fibre Solutions, Australian Paper and Circa. Special thanks to Maheshi Udugama (Monash University) for advice and discussions regarding electrophoresis.

Appendix A. Supplementary material

Supplementary data to this article can be found online at https://doi.org/10.1016/j.jcis.2019.01.017.

References

[1] J.A. Armstrong, J.R. Schulz, Agarose gel electrophoresis, in: Current Protocols Essential Laboratory Techniques, 2008.
[2] A. Tiselius, A new apparatus for electrophoretic analysis of colloidal mixtures, Trans. Faraday Soc. 33 (1937) 524–531.
[3] M.J. Gordon et al., Capillary electrophoresis, Science 242 (4876) (1988) 224–228.
[4] D. Voytas, Agarose gel electrophoresis, Curr. Protoc. Mol. Biol. 51 (1) (2000) 2.5A.1–2.5A.9.
[5] V.L. Royse, D.M. Jensen, Development of an agarose gel electrophoresis technique for determining alpha-amylase isoenzymes, Clin. Chem. 30 (3) (1984) 387–390.
[6] J. Chory, J.D. Pollard, Separation of small DNA fragments by conventional gel electrophoresis, Curr. Protoc. Mol. Biol. 47 (1) (1999) 2.7.1–2.7.8.
[7] R. Bravo, CHAPTER 1 – two-dimensional gel electrophoresis: a guide for the beginner, in: J.E. Celis, R. Bravo (Eds.), Two-Dimensional Gel Electrophoresis of Proteins, Academic Press, 1984, pp. 3–36.
[8] M. Friedman, Chemistry, biochemistry, and safety of acrylamide. A review, J. Agric. Food. Chem. 51 (16) (2003) 4504–4526.
[9] R. Westermeier, Electrophoresis, in: Electrophoresis in Practice: A Guide to Methods and Applications of DNA and Protein Separations, 2005, p. 16.
[10] T. Abitbol et al., Nanocellulose, a tiny fiber with huge applications, Curr. Opin. Biotechnol. 39 (2016) 76–88.
[11] D. Klemm et al., Cellulose: fascinating biopolymer and sustainable raw material, Angew. Chem. Int. Ed. 44 (22) (2005) 3358–3393.
[12] A. Isogai, T. Saito, H. Fukuzumi, TEMPO-oxidized cellulose nanofibers, Nanoscale 3 (1) (2011) 71–85.
[13] L. Mendoza et al., Gelation mechanism of cellulose nanofibre gels: a colloids and interfacial perspective, J. Colloid Interf. Sci. 509 (2018) 39–46.
[14] L. Jowkarderis, T.G.M. van de Ven, Intrinsic viscosity of aqueous suspensions of cellulose nanofibrils, Cellulose 21 (4) (2014) 2511–2517.
[15] L. Jowkarderis, T.G.M. van de Ven, Rheology of semi-dilute suspensions of carboxylated cellulose nanofibrils, Carbohydr. Polym. 123 (2015) 416–423.
[16] E. Lasseuguette, D. Roux, Y. Nishiyama, Rheological properties of microfibrillar suspension of TEMPO-oxidized pulp, Cellulose 15 (3) (2008) 425–433.
[17] O. Nechyporchuk, M.N. Belgacem, F. Pignon, Rheological properties of micro-/nanofibrillated cellulose suspensions: wall-slip and shear banding phenomena, Carbohydr. Polym. 112 (Supplement C) (2014) 432–439.
[18] O. Nechyporchuk, M.N. Belgacem, F. Pignon, Concentration effect of TEMPO-oxidized nanofibrillated cellulose aqueous suspensions on the flow instabilities and small-angle X-ray scattering structural characterization, Cellulose 22 (4) (2015) 2197–2210.
[19] M. Hakalahti et al., Effect of interfibrillar PVA bridging on water stability and mechanical properties of TEMPO/NaClO2 oxidized cellulosic nanofibril films, Carbohydr. Polym. 126 (2015) 78–82.
[20] H. Zhang et al., Cellulose anionic hydrogels based on cellulose nanofibers as natural stimulants for seed germination and seedling growth, J. Agric. Food Chem. 65 (19) (2017) 3785–3791.
[21] S.M.F. Kabir et al., Cellulose-based hydrogel materials: chemistry, properties and their prospective applications, Prog. Biomater. 7 (3) (2018) 153–174.
[22] S. Boufi et al., Nanofibrillated cellulose as an additive in papermaking process: a review, Carbohydr. Polym. 154 (2016) 151–166.
[23] P. Gatenholm, D. Klemm, Bacterial nanocellulose as a renewable material for biomedical applications, MRS Bull. 35 (3) (2011) 208–213.
[24] P.R. Sharma et al., Nanocellulose from spinifex as an effective adsorbent to remove cadmium(II) from water, ACS Sustain. Chem. Eng. 6 (3) (2018) 3279–3290.
[25] S. Gustafsson, L. Manukyan, A. Mihranyan, Protein-nanocellulose interactions in paper filters for advanced separation applications, Langmuir 33 (19) (2017) 4729–4736.
[26] M. Vuoriluoto et al., Control of protein affinity of bioactive nanocellulose and passivation using engineered block and random copolymers, ACS Appl. Mater. Interf. 8 (8) (2016) 5668–5678.
[27] J.-M. Malho et al., Enhanced plastic deformations of nanofibrillated cellulose film by adsorbed moisture and protein-mediated interactions, Biomacromolecules 16 (1) (2015) 311–318.
[28] C. Xu, D.O. Carlsson, A. Mihranyan, Feasibility of using DNA-immobilized nanocellulose-based immunoadsorbent for systemic lupus erythematosus plasmapheresis, Colloids Surf. Biointerf. 143 (2016) 1–6.
[29] C. Uth et al., A chemoenzymatic approach to protein immobilization onto crystalline cellulose nanoscaffolds, Angew. Chem. Int. Ed. 53 (46) (2014).
[30] V. Kuzmenko et al., Universal method for protein bioconjugation with nanocellulose scaffolds for increased cell adhesion, Mater. Sci. Eng., C 33 (8) (2013) 4599–4607.
[31] N.E. Zander et al., Metal cation cross-linked nanocellulose hydrogels as tissue engineering substrates, ACS Appl. Mater. Interf. 6 (21) (2014) 18502–18510.
[32] J. Leppiniemi et al., 3D-printable bioactivated nanocellulose-alginate hydrogels, ACS Appl. Mater. Interf. 9 (26) (2017) 21959–21970.
[33] G. Mondragon et al., Bionanocomposites based on gelatin matrix and nanocellulose, Eur. Polym. J. 62 (2015) 1–9.
[34] J. Liu et al., Development of nanocellulose scaffolds with tunable structures to support 3D cell culture, Carbohydr. Polym. 148 (2016) 259–271.
[35] A. Müller et al., The biopolymer bacterial nanocellulose as drug delivery system: investigation of drug loading and release using the model protein albumin, J. Pharm. Sci. 102 (2) (2013) 579–592.
[36] A. Müller et al., Loading of bacterial nanocellulose hydrogels with proteins using a high-speed technique, Carbohydr. Polym. 106 (2014) 410–413.
[37] A. Razaq et al., High-capacity conductive nanocellulose paper sheets for electrochemically controlled extraction of DNA oligomers (Conductive Nanocellulose for Extraction of DNA), PLoS One 6 (12) (2011) e29243.
[38] L. Mendoza et al., Effects of fibre dimension and charge density on nanocellulose gels, J. Colloid Interf. Sci. 525 (2018) 119–125.
[39] K. Hunger et al., Investigation of cross-linked and additive containing polymer materials for membranes with improved performance in pervaporation and gas separation, Membranes 2 (4) (2012) 727–763.
[40] I. Braccini, S. Pérez, Molecular basis of Ca2+-induced gelation in alginates and pectins: the egg-box model revisited, Biomacromolecules 2 (4) (2001) 1089–1096.
[41] J. Schmitt et al., TEMPO-oxidised cellulose nanofibrils; probing the mechanisms of gelation via small angle X-ray scattering, PCCP 20 (23) (2018) 16012–16020.
[42] S. Suenaga, M. Osada, Self-sustaining cellulose nanofiber hydrogel produced by hydrothermal gelation without additives, ACS Biomater. Sci. Eng. 4 (5) (2018) 1536–1545.
[43] E. Valeur, M. Bradley, Amide bond formation: beyond the myth of coupling reagents, Chem. Soc. Rev. 38 (2) (2009) 606–631.
[44] H. Orelma et al., CMC-modified cellulose biointerface for antibody conjugation, Biomacromolecules 13 (4) (2012) 1051–1058.
[45] R.K. Mylavarapu et al., Boric acid catalyzed amidation in the synthesis of active pharmaceutical ingredients, Org. Process Res. Dev. 11 (6) (2007) 1065–1068.
[46] M.T. Sabatini, L.T. Boulton, T.D. Sheppard, Borate esters: simple catalysts for the sustainable synthesis of complex amides, Sci. Adv. 3 (9) (2017).
[47] K. Syverud et al., Controlling the elastic modulus of cellulose nanofibril hydrogels—scaffolds with potential in tissue engineering, Cellulose 22 (1) (2015) 473–481.
[48] L. Mendoza et al., Carboxylated nanocellulose foams as superabsorbents, J. Colloid Interf. Sci. 538 (2019) 433–439.